Journal of Power and Energy Systems

Vol. 2, No. 6, 2008

Thermoelectric Power Conversion System Combined with LNG Vaporizer*

Mitsuru KAMBE**, Ryo MORITA**, Kazuyuki OMOTO***, Yasuhiro KOJI***, Tatsuo YOSHIDA**** and Koji NOISHIKI****

**Central Research Institute of Electric Power Industry (CRIEPI)
2-11-1, Iwado-kita, Komae-shi, Tokyo, 201-8511 JAPAN
E-mail: kambe@criepi.denken.or.jp
***The Kansai Electric Power Co., Inc.
3-11-20, Nakoji, Amagasaki, Hyogo, 661-0974 JAPAN
**** Kobe Steel, Ltd.
2-3-1, Shinhama, Arai-cho, Takasago-city, Hyogo, 676-8670 JAPAN

Abstract

A conceptual design of the thermoelectric power conversion system combined with open rack type LNG (liquefied natural gas) vaporizer to make use of cold heat of LNG is presented. The system performance analysis has been made based on the thermoelectric module performance data obtained at the cryogenic thermoelectric (CTE) test rig which could realize temperature and fluid dynamic condition of the open rack type LNG vaporizer. Conventional bismuth-telluride thermoelectric modules were tested, however, each module is encapsulated in the stainless steel container to achieve water proof. Electricity production cost evaluation of the system is also discussed.

Key words: Liquefied Natural Gas, LNG, LNG Vaporizer, Open Rack Type Vaporizer, ORV, Cryogenic, Thermoelectric, Bismuth-Telluride

1. Introduction

Liquefied natural gas (LNG) is essentially clean energy and its consumption is increasing world wide because natural gas combustion produces less carbon dioxide than oil. The LNG power station is equipped with the LNG vaporizers to evaporate LNG of –160ºC. LNG vaporizer is designed to re-gasify cryogenic LNG by heat exchange. There are two basic types of LNG vaporizer; one is open rack type (ORV) and the other submerged combustion type. ORV utilizes seawater as a heat source. Seawater flows down on the outside surface of the aluminum heat exchanger panel and vaporizes inside LNG of the panel. In this process cold heat of LNG is disposed to seawater. An attention was focused to make use of this temperature gradient i.e. –160ºC to room temperature by thermoelectric power conversion system (TE system).

The TE system is so far applied to the temperature gradient from room temperature to higher temperature, usually several hundreds degrees Celsius. The TE system features no moving parts and reliable performance. It is demonstrated by most of the spacecrafts of deep space missions launched by the USA since 1960s. In this case silicon-germanium (SiGe) or lead-telluride (PbTe) thermoelectric modules (TE modules) were heated by the radioisotope heat source of plutonium 238 (Pu_{238}) or strontium 90 (St_{90}). Hot side temperature of this SiGe TE module is over 800ºC. For terrestrial applications, however, TE module is usually applied to heat source of less than 600ºC, in other word, the available heat source in the terrestrial system is usually below 600ºC. Several TE semiconductors are available depending on the operating temperature. For example, silicon-germanium (SiGe)

*Received 15 July, 2008 (No. 08-0479)
[DOI: 10.1299/jpes.2.1304]

performs best at the high temperatures (over 600ºC), while zinc-antimony (ZnSb) achieves greatest effectiveness at intermediate temperatures (200-500ºC), and bismuth-telluride (BiTe) has excellent performance at lower temperatures (room temperature to 200ºC). BiTe can also function as spot coolers when operated in reverse. On the other hand, published papers on the TE module performance at the temperature gradient from room temperature to cryogenic temperature are scarcely available.

This paper presents a conceptual design of the TE system combined with open rack type LNG vaporizer. The system performance analysis has been made based on the TE module performance data obtained at the cryogenic thermoelectric (CTE) test rig which could realize temperature and fluid dynamic condition of the open rack type LNG vaporizer. Conventional BiTe TE modules were tested, however, each module is encapsulated in the stainless steel container to achieve water proof. Electricity production cost evaluation of this TE system is discussed as well.

2. Thermoelectric Module Performance in Cryogenic Temperature Range

2.1 Encapsulated thermoelectric module

At the beginning of this research activity, our primary concern was the TE module performance in the cryogenic temperature range. Conventional BiTe TE modules were tested, however, each module is encapsulated in the stainless steel container to keep away from humidity and to achieve water proof. The TE module (type L) adopted is a 111 couples skeleton type, measures 40×35 mm and 3 mm thick, manufactured by Ferrotec Corporation, as shown in Fig.1. The encapsulated TE module in which this TE module is encased is shown in Fig.2. The container, measures 55×51 mm and 11 mm thick, is originally developed for high temperature SiGe TE modules by the joint research of CRIEPI, Hitachi Powdered Metals Co., Ltd. and NEDO [1]. It features vacuum tight and heat resistant up to 700ºC. Because inside of the container is kept vacuum, the stainless steel (SUS316) top container of 0.1 mm thick always exerts pressing load on the TE module by the difference pressure of 0.1 MPa, which results in reduction of thermal contact resistance in the container and accordingly enhance module performance independent of the operating temperature.

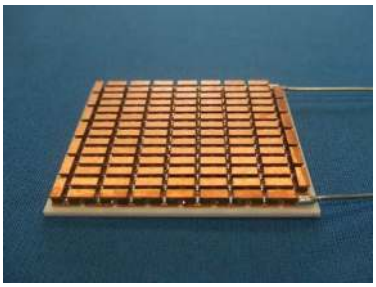

Fig.1 TE module (type L)

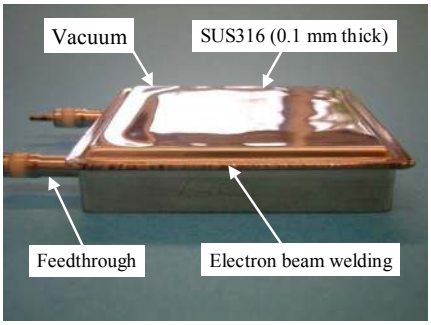

Fig.2 Encapsulated TE module

2.2 Module performance in the vacuum chamber

The initial attempt was to measure the encapsulated module performance in the cryogenic temperature range. Measurement has been done in the vacuum chamber in which a heater block and cold plate as well as instrumentations are equipped, as shown in Fig. 3. Due to safety reasons, liquefied nitrogen (–196ºC) is adopted instead of LNG (–160ºC) to cool the cold plate. The vacuum chamber could avoid icing on the TE module during measurement. The external electrical resistance of the circuit was adjusted as 1Ω which is equal to the module internal resistance because the maximum module power is available in this condition. Thermocouples adopted were K type (class 1) with the accuracy ±1.5 K in

the range down to −60ºC. Calibration using liquid nitrogen (–196ºC), however, ensured that it has practically sufficient accuracy in the cryogenic temperature range of interest.

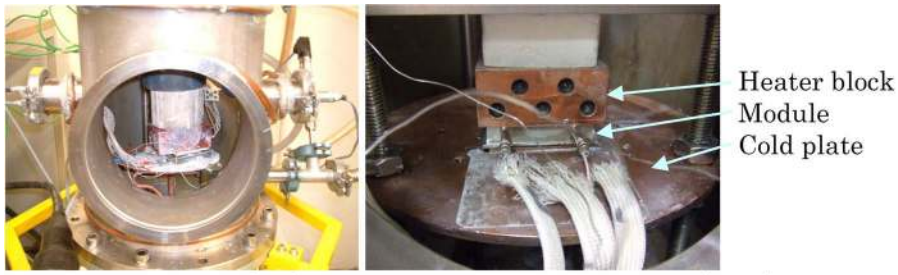

Vacuum chamber (left) and inside view of the chamber (right)

Fig. 3 Vacuum chamber for module performance measurement

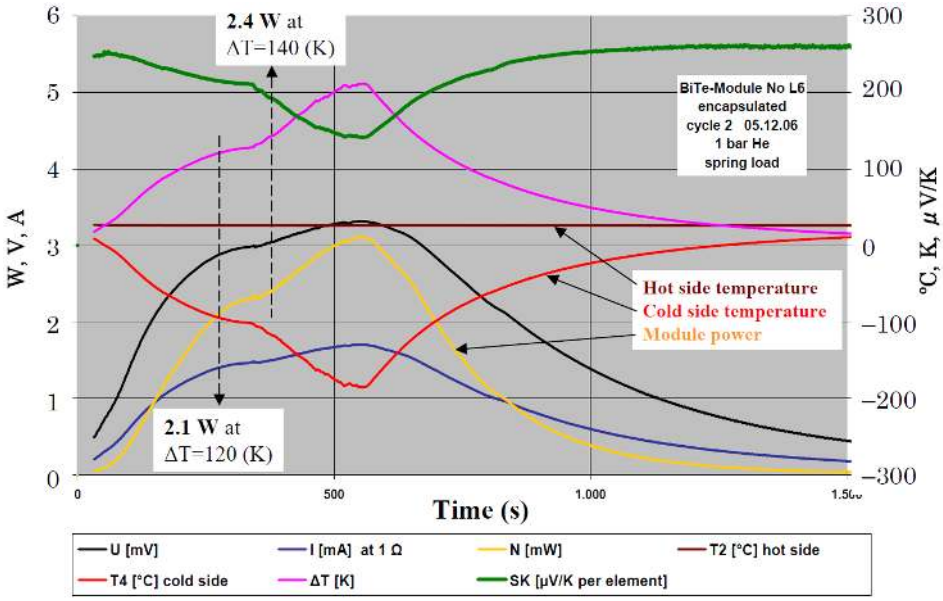

Fig.4 Encapsulated TE module data in the vacuum chamber (Module L 06)

Table 1 Encapsulated TE module performance (Type L)

Module ID	Encapsulated module power (W) and conversion efficiency η (%)			
	ΔT=120 K		ΔT=140 K	
L 27	2.2 W	(3.9 %)	2.9 W	(4.4 %)
L 14	2.4 W	(4.2 %)	3.1 W	(4.7 %)
L 05	1.8 W	(3.2 %)	2.3 W	(3.6 %)
L 10	2.2 W	(3.9 %)	2.7 W	(3.9 %)
L 01	1.9 W	(3.4 %)	2.5 W	(3.7 %)
L 06	2.1 W	(3.8 %)	2.4 W	(3.6 %)
Average	**2.1 W**	**(3.7 %)**	**2.7 W**	**(4.0 %)**

One of the results is shown in Fig.4. This module provides 2.4 W at container hot side 20ºC and cold side –120ºC (ΔT=140 K) which is near to our temperature range of interest. As discussed later in the chapter 4.1, the operating temperature of the encapsulated module in our proposed design is; container hot side –2ºC and cold side –142ºC (ΔT=140 K) at the bottom of the TE module section, and container hot side 0ºC and cold side –120ºC (ΔT=120 K) at the top of the TE module section. Module performance data of type L are summarized in Table 1. Conversion efficiency η in the table is calculated as follows.

$$\eta = (P \times R_{Mod}) / (A \times \Delta T_{Mod}) \quad \text{--- (1)}$$

where P Module power

R_{Mod} Thermal resistance of the encapsulated TE module $=3.0\times10^{-3}$ (m^2K/W)

A Module area $=1.4\times10^{-3}$ (m^2)

ΔT_{Mod} Temperature gradient of the encapsulated TE module

Further investigation on the module performance in cryogenic temperature range has been made on the other TE module. TE modules tested this time (type N) were same dimension as the former, also conventional module manufactured by Ferrotec Corporation, however, BiTe composition is different. Not only the encapsulated module performance, but also module performance without container is measured. Typical data are shown in Figs. 5 and 6. Module performance data of type N are summarized in Table 2.

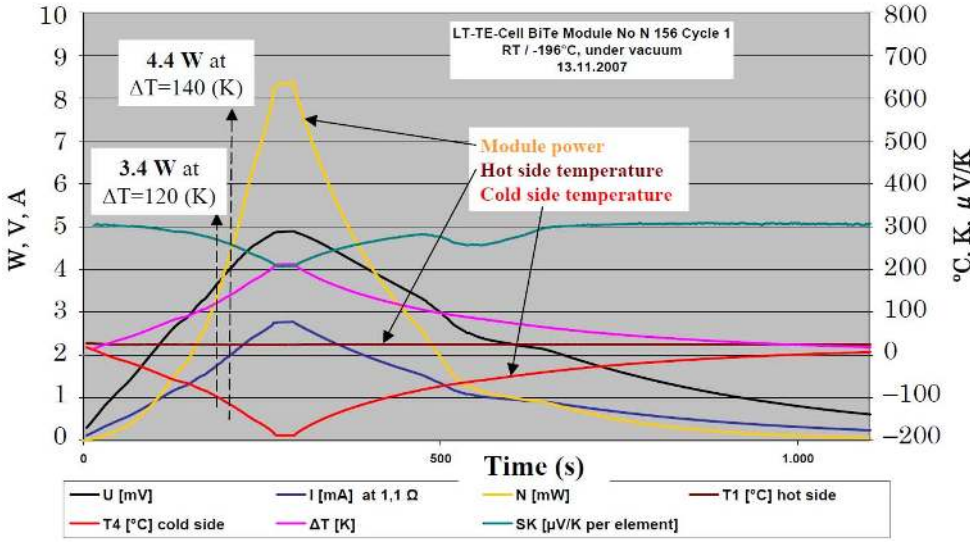

Fig.5 TE module data without container in the vacuum chamber (Module N 156)

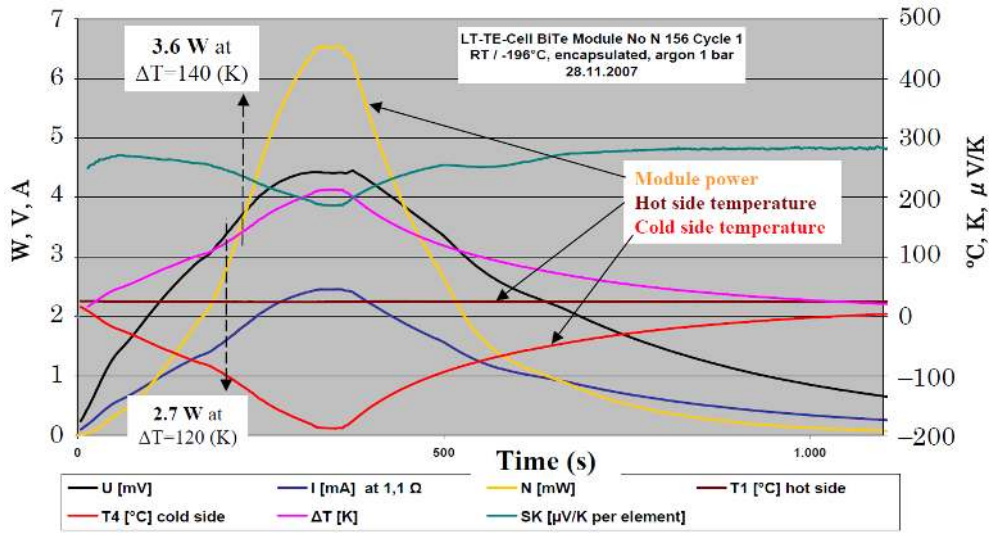

Fig.6 Encapsulated TE module data in the vacuum chamber (Module N 156)

Table 2 TE module performance (Type N)

Module ID	Module power (W) and conversion efficiency η (%)			
	ΔT=120 K		ΔT=140 K	
	without container	/ encapsulated	without container	/ encapsulated
N 156	3.4 W	2.7 W (4.8 %)	4.4 W	3.6 W (5.5 %)
N 158	3.8 W	2.5 W (4.5 %)	5.5 W	3.4 W (5.2 %)
N 144	3.9 W	2.2 W (3.9 %)	4.8 W	3.1 W (4.7 %)
N 150	3.3 W	2.2 W (3.9 %)	4.3 W	2.9 W (4.4 %)
N 153	4.0 W	– *	4.9 W	– *
N 159	3.7 W	2.3 W (4.1 %)	4.8 W	3.0 W (4.6 %)
Average	3.7 W	2.4 W (4.2 %)	4.8 W	3.2 W (4.9 %)

*) Failure to save data

Due to the existence of thermal resistance of the container itself, the encapsulated module power is about 60 to 80% of that without container. Because the module power is roughly proportional to the square of the temperature gradient imposed to the TE semiconductor, thermal resistance of the container might be 10 to 20% of the total thermal resistance of encapsulated module. The latter module (type N) provided better performance than that of the former (type L). As for type N modules, performance data in the higher temperature range is also available. For example, it provided 2.5 W at module hot side (without container) 140ºC and cold side 20ºC (ΔT=120 K), which is less than that of corresponding data in Table 2 (3.7 W in average). Now we have learned that performance of conventional BiTe TE modules in the cryogenic temperature range seems to be better than that in the higher temperature range (i.e. room temperature to 200ºC). Improvement of the TE semiconductor material could enhance module performance. It is left for future research and development.

3. Proposed Thermoelectric Power Conversion System combined with LNG Vaporizer

3.1 Conventional open rack vaporizer (ORV) design

LNG vaporizer is designed to re-gasify cryogenic LNG by heat exchange. There are two basic types of LNG vaporizer; one is open rack type (ORV) and the other submerged combustion type. A schematic of the conventional ORV [2] is shown in Fig. 7. The ORV utilizes seawater as a heat source. Seawater flows down on the outside surface of the aluminum heat transfer tube panel and vaporizes inside LNG of the tube. Detail of the tube is shown in Fig. 8 [2]. LNG enters into the tube at the bottom, then vaporized and heated as coming up. The vaporizing zone and heating zone have different cross section to reduce the ice layer height and thickness in the former and to achieve greater heat transfer in the latter. The overall tube length is 6 or 8 m. As shown in the figure, the ORV tube has several fins parallel to the axis both on the outside and inside to enhance heat transfer. In addition, twisted cross bar is also inserted to accelerate turbulent flow.

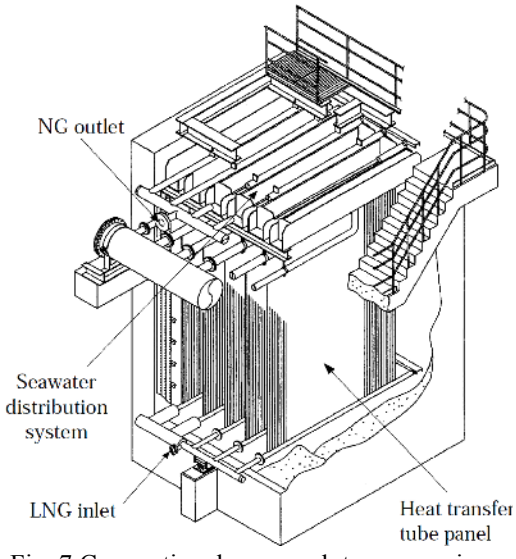

Fig. 7 Conventional open rack type vaporizer

In this process cold heat of LNG is disposed to seawater. An attention was focused to

make use of this temperature gradient i.e. –160ºC to room temperature by thermoelectric power conversion system (TE system).

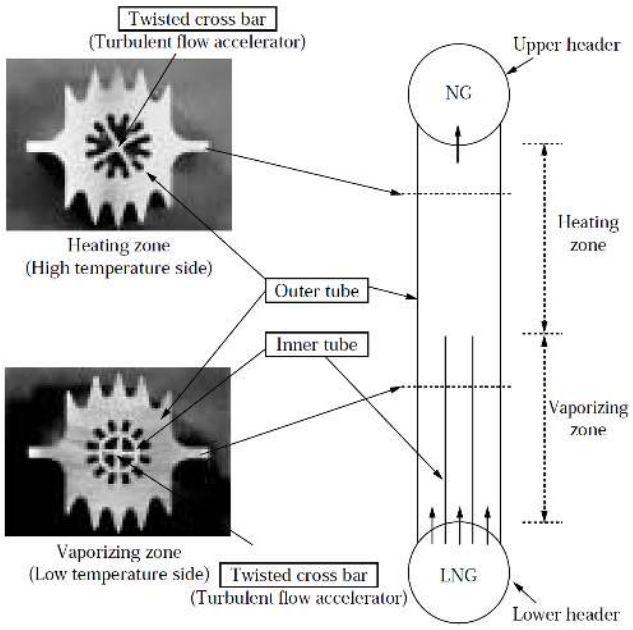

Fig. 8 ORV heat transfer tube detail

3.2 Proposed thermoelectric power conversion system for ORV

TE module power is roughly proportional to the square of the temperature gradient imposed to the TE semiconductor. In view of this, the best location for TE module is the bottom of the ORV tube where LNG of –160ºC just enters and coming up. According to our operational experience on the conventional type ORV, the lower region of the tube will have ice layer of sea water, especially in winter. This ice layer has extremely low thermal conductivity, therefore increases the thermal resistance of the tube, and accordingly reduces the ORV performance. Heat transfer analysis using ORV design cord by Kobe Steel revealed that ice layer in the bottom of the tube is 1 m high and about 10 mm thick. If we put TE modules in this region, ice formation would be avoided while electrical power could be available. Then our design policy of the TE system for ORV is to get electrical power without any influence on the ORV performance. In addition it should be as compatible as that of conventional ORV so as that this TE system is easily introduced in the market.

Proposed TE system design is illustrated in Fig. 9. The TE module section, however, is 2 m long on which a transition element is attached to connect conventional finned ORV tube (4.8 m long) and the TE module section of rectangular cross section smoothly, and to stabilize water flow over the TE module section. Although the overall length of 7 m is 1 m longer than that of the standard one, it is optimized in view of greater electrical power of the TE system with a slight influence on the conventional ORV installation.

Horizontal cross section of the TE module section is shown in Fig. 10. Conventional aluminum heat transfer tube panel consists of several tenths of ORV tubes placed in a line with a pitch of 54.5 mm. This tube pitch is also kept in our proposed design. In each tube, 52 TE modules are attached on two sides (i.e. 26 modules×2 sides). Gaps of 4.5 mm width are filled with thermal insulation to avoid thermal shortcut between the tube surface and water because it would result in reduction of the TE module power.

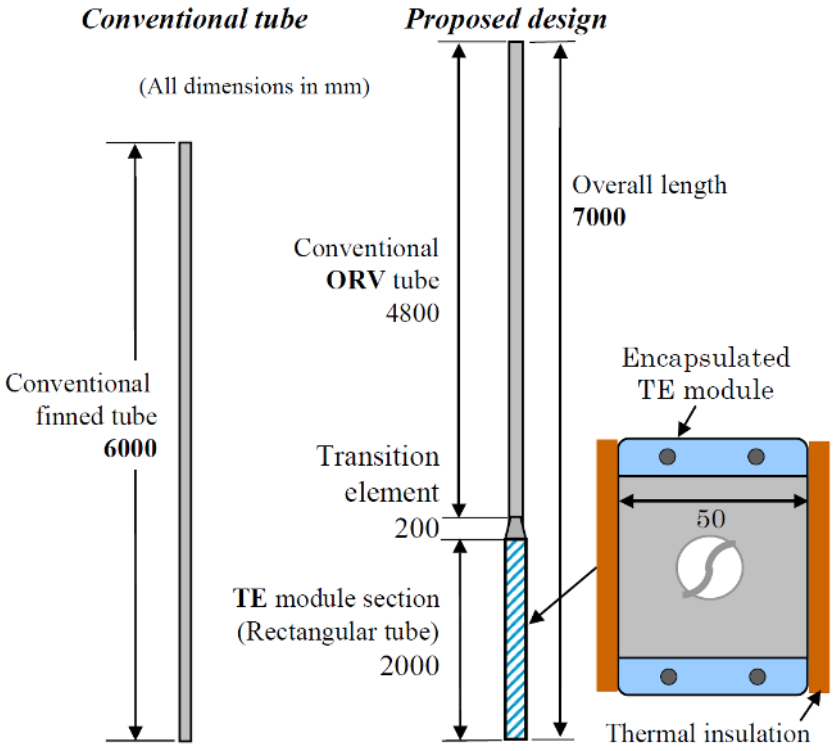

Fig. 9 Proposed TE system design

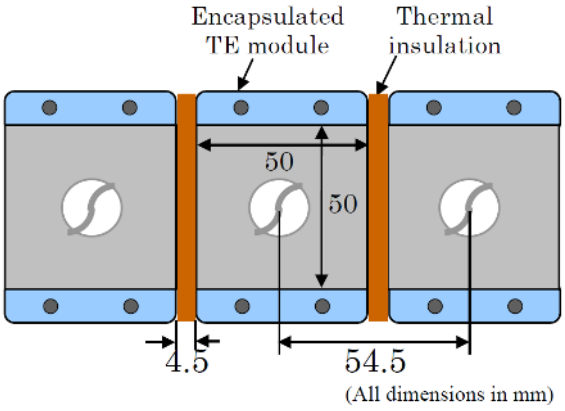

Fig. 10 Horizontal cross section of the TE module section (only 3 tubes shown)

3.3 Fluid dynamic optimization of the transition element

Fluid dynamic optimization of the transition element has been conducted using a full scale aluminum specimen as shown in Fig. 11. Detail of the transition element is shown in Fig. 12. This is a 3-dimensional NC machined element of 200 mm long to connect conventional ORV tube and the TE module section smoothly. Fluid dynamic test demonstrated that water is well stabilized and flows down perfectly over the TE module section as shown in Fig. 13. This test, however, was conducted on the single tube. Actually tubes are arranged with a pitch of 54.5 mm as shown in Fig. 10, therefore water flows down between the conventional finned tubes would spread horizontally at the top of the TE module section where thermal insulation interrupts the flow. Control of this secondary flow could be achieved by a 3-dimensional flow test using multi tubes. It is left for future

research and development.

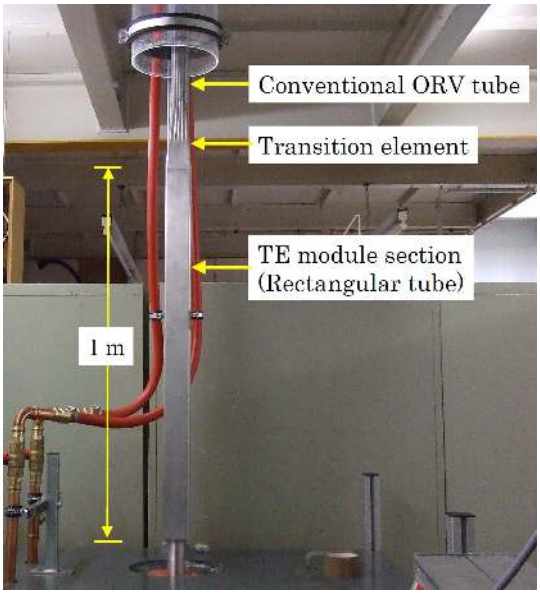

Fig. 11 ORV tube setup for the fluid dynamic test

Fig. 12 Detail of the transition element

Fig. 13 Water flow on the transition element

3.4 Module performance at the cryogenic thermoelectric (CTE) test rig

In order to achieve thermoelectric system performance test, the cryogenic thermoelectric (CTE) test rig was constructed as shown in Figs. 14 and 15. Due to restriction of the laboratory, the overall length of the tube is 4 m instead of actual length of our design (7 m). However, it is sufficient for the purpose of the experiment because water supplied at the top of the ORV tube would accelerate its velocity as flows down on the tube surface and attain its maximum velocity (approximately 3 m/s) within 1 m from the top. Therefore we are sure that this test rig could achieve actual water flow situation on the TE module section. Liquefied nitrogen (–196ºC) is adopted instead of LNG (–160ºC) due to safety reasons.

Figures 16 and 17 show the TE module section on which an encapsulated TE module (L06) and 7 dummy TE modules (only containers without TE modules) are provided. In our proposed TE system design, however, 52 TE modules (26 modules×2 sides) could be attached on the TE module section of each ORV tube based on the following estimation.

Encapsulated TE module length: 70 mm long including feedthrough (refer to Fig. 2)

Encapsulated TE modules pitch on the TE module section: 70+5=75 mm

Number of TE modules on one of the sides of the TE module section: 2000/75=26

Fewer TE modules (including dummy TE modules) on the CTE test rig is allowed to check water flow on the TE module section.

Thermocouples are attached to both the hot and cold sides of the encapsulated TE module. Thermocouples are also attached to the hot side of the typical dummy containers to monitor the water temperature. Thermocouples adopted were K type (class 1), same as those in the module performance tests (refer to chapter 2.2).

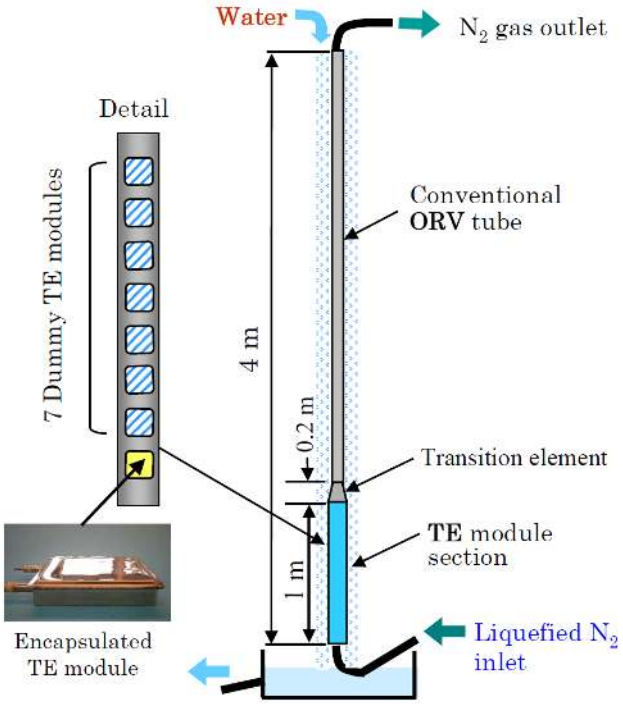

Fig. 14 Schematic of the CTE test rig

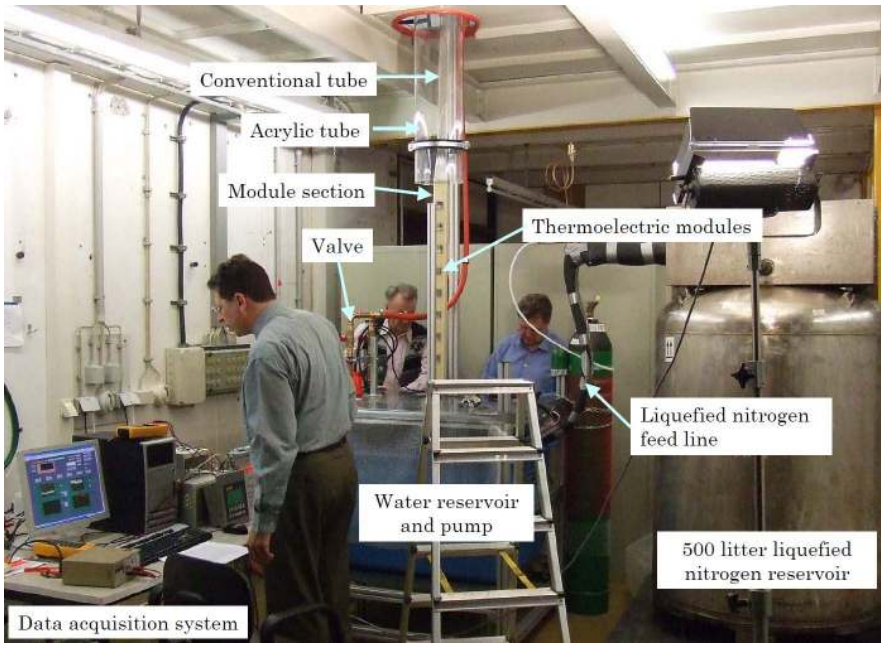

Fig. 15 Overview of the CTE test rig

As a thermal insulation, filler material which solidifies by chemical reaction, trade name Zelupur manufactured by Zelu Chemie GmbH was adopted. This is a thermal insulation widely adopted for housing construction and automobile industry. Power cables of the TE module as well as water proof connectors are sealed in the thermal insulation layer. The TE module section has a flat surface so as that water is well stabilized and flows down perfectly over the TE module section.

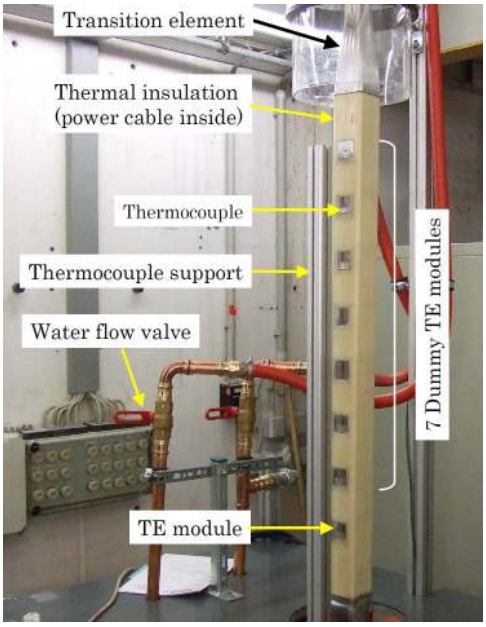

Fig. 16 TE module section of the CTE test rig (side view)

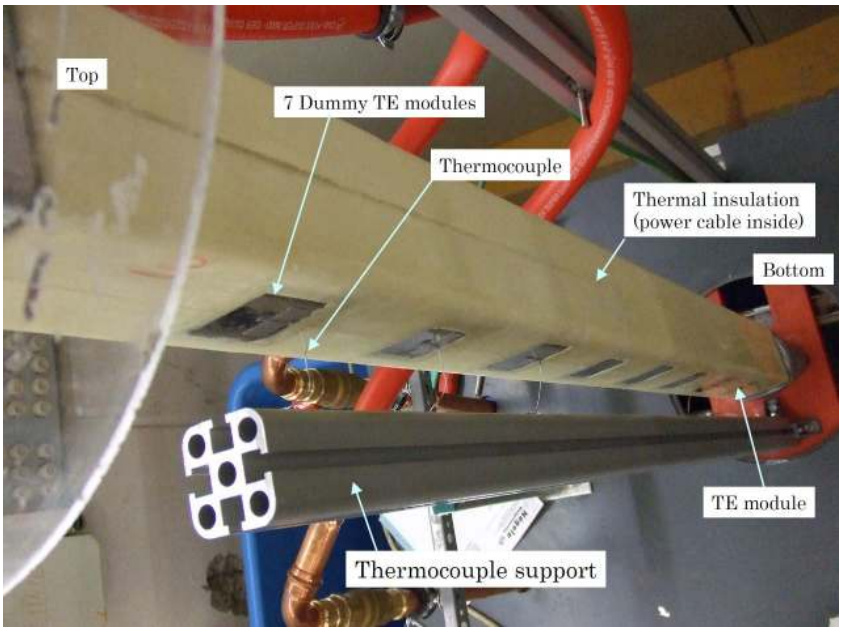

Fig. 17 TE module section of the CTE test rig (vertical view)

Module performance data at the CTE test rig is presented in Fig. 18. Test has been conducted by circulating water of room temperature around the tube while supplying liquefied nitrogen into the tube, then module power increases as increasing temperature difference between the hot and cold side of the TE module. The encapsulated TE module (L06) provides electrical power of 1.97 W (η=3.5%) at ΔT=120 K and 2.11 W (η=3.2%) at ΔT=140 K. As discussed later in the chapter 4.1, the operating temperature of the encapsulated module in our proposed design is; container hot side –2ºC and cold side –142ºC (ΔT=140 K) at the bottom of the TE module section, and container hot side 0ºC and cold side –120ºC (ΔT=120 K) at the top of the TE module section. Due to restriction of the CTE test rig, water temperature was about 20 K higher than that of the proposed design, however, it is not so important because module power is roughly proportional to the square

of the temperature difference while not significant change is foreseen on the BiTe properties in such a slight temperature shift. The electrical power of the module L06 available at CTE test rig is slightly lower than that measured in the vacuum chamber (2.1 W at ΔT=120 K and 2.4 W at ΔT=140 K, as shown in Table 1). This might be responsible for shortcut of the heat through the sides of module container and thermal insulation. Test run using N type module, which presented better performance in the vacuum chamber as shown in table 2, would results in greater electrical power, however, it is not conducted yet.

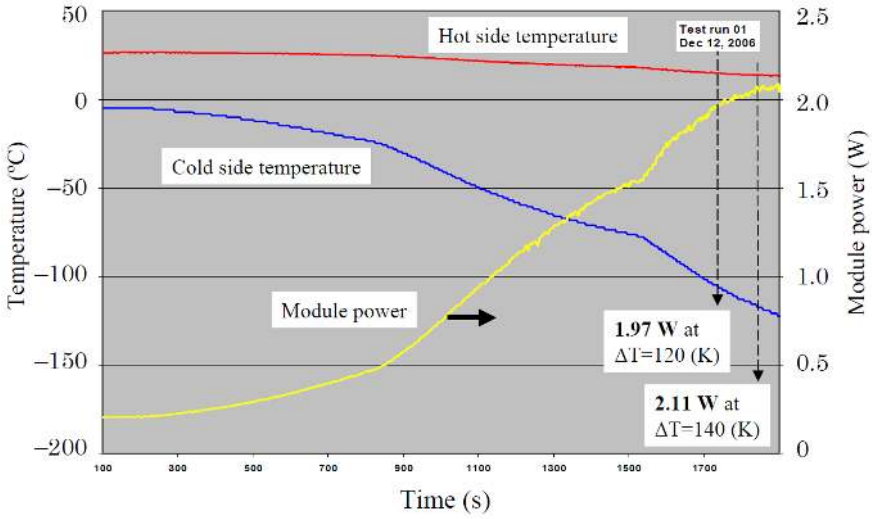

Fig. 18 Module performance at the CTE test rig (Module L06)

4. Performance and Cost Evaluation of the System

4.1 Analytical model

Based on the data obtained in the vacuum chamber and CTE test rig, TE system performance of our proposed design shown in Fig. 9 has been analyzed. A performance breakdown of the LNG plant without/with TE system is shown in Table 3.

Table 3 Performance breakdown of the LNG plant without/with TE system

LNG nominal flow rate	120 (t/h)
Sea water nominal flow rate	4000 (t/h)
LNG inlet temperature	−155 (°C)
Sea water inlet temperature	10 (°C)
ORV tube overall length (without/with TE system)	6 (m)/ 7 (m)
Number of ORV tubes	540 (=90 tubes×6 panels)

The TE system performance is calculated by the heat transfer model shown in Fig. 19 where the following symbols appear.

ΔT Temperature gradient between LNG and sea water
=159 (K) at the bottom and 136 (K) at the top of the TE module section

Q Total heat passes through the TE module section= $Q_{Mod} + Q_{Ins}$

Q_{Mod} Heat passes through the encapsulated TE module

Q_{Ins} Heat passes through the thermal insulation

R_W Thermal resistance of sea water = $1/h_W$

R_{Mod} Thermal resistance of the encapsulated TE module =3.0×10^{-3} (m^2K/W)

R_{Ins} Thermal resistance of the thermal insulation
= $t/\lambda=10\times10^{-3}$ (m)/1.0 (W/mK) =10×10^{-3} (m^2K/W)

R_{Ex} Thermal resistance of the tube of TE module section
$= t/\lambda = 0.017\ (m)/200\ (W/mK) = 0.09\times10^{-3}\ (m^2K/W)$
R_C Thermal resistance of LNG $= 1/h_C$
R_{Eq} Equivalent thermal resistance of the module and insulation
R Overall thermal resistance of the TE module section $=R_W+R_{Eq}+R_{Ex}+R_C$
A Total area of the TE module section
$=2\ (m\ long)\times0.05\ (m\ wide)\times2\ (sides)\times540\ (tubes)=108\ (m^2)$
A_{Mod} Area of the encapsulated TE module
$=40\ (mm)\times35\ (mm)\times52\ (modules)\times540\ (tubes)$
$=1.4\times10^{-3}\ (m^2)\times52\ (modules)\times540\ (tubes)=39.3\ (m^2)$
A_{Ins} Area of the thermal insulation $=A-A_{Mod}=108-39.3=68.7\ (m^2)$
h_W Heat transfer coefficient of sea water at the TE module section
h_C Heat transfer coefficient of LNG at the TE module section

As shown in Fig. 17, outside surface of the TE module section is almost flat, therefore the heat transfer coefficient of sea water h_W was deduced from that of water flow over the vertical flat plate. While the heat transfer coefficient of LNG h_C was obtained experimentally by Kobe Steel using actual ORV tube and LNG.

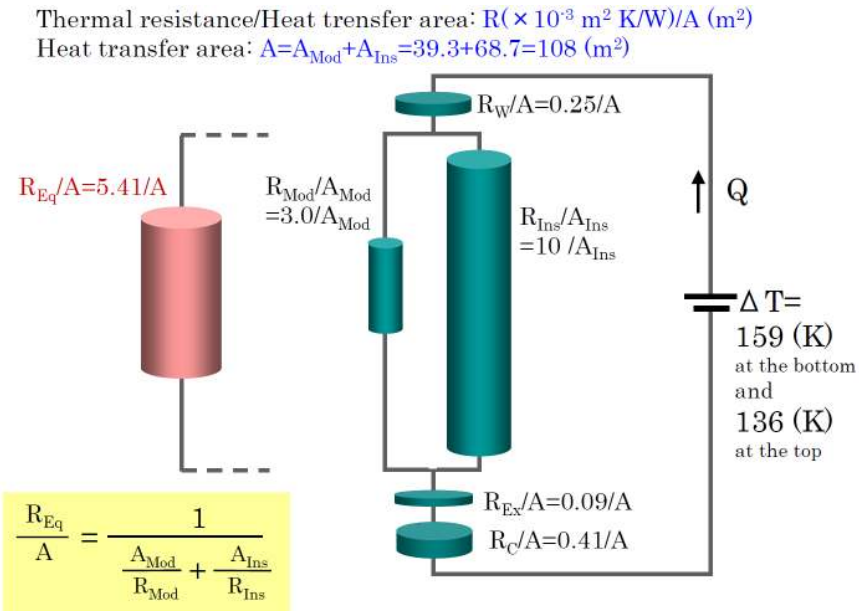

Fig. 19 Heat transfer model of the proposed TE system

As shown above, thermal conductivity of the insulation (Zelupur) was supposed to be 1.0 (W/mK). The gaps of 4.5 mm width between tubes are also filled with the same insulation (Fig. 10). In the above model, heat passes through only 2 sides of the TE module section where TE modules are attached are taken into account, because other 2 sides are almost adiabatic. The purpose of the work here is to estimate temperature gradient imposed on the encapsulated TE module in the proposed system. The following calculations suggest that 88% of ΔT is imposed on the encapsulated TE module itself.

$$R = R_W + R_{Eq} + (R_{Ex} + R_C) = [(0.25+5.41+(0.09+0.41)]\times10^{-3}$$
$$= (0.25+5.41+0.50)\times10^{-3} = 6.16\times10^{-3}\ (m^2K/W) \quad \text{--- (2)}$$
$$R_{Eq}/R = 5.41/6.16 = 0.88 \quad \text{--- (3)}$$

According to the following estimation, 66% of the total heat flux in the TE module

section passes through the encapsulated TE modules, and the rest passes through the insulation.

$$R_{Mod}/A_{Mod} = 3.0\times10^{-3}\ (m^2K/W)/39.3\ (m^2) = 76.3\times10^{-6}\ (K/W) \quad \text{--- (4)}$$

$$R_{Ins}/A_{Ins} = 10\times10^{-3}\ (m^2K/W)/68.7\ (m^2) = 146\times10^{-6}\ (K/W) \quad \text{--- (5)}$$

$$Q_{Mod}:Q_{Ins} = 146/(76.3+146):76.3/(76.3+146) = 0.66:0.34 = 66\%:34\% \quad \text{--- (6)}$$

Calculated temperature distribution in the proposed system is presented in Fig. 20. Water inlet temperature 10ºC and LNG inlet temperature –155ºC are design conditions suggested by Kobe steel. Although the latter temperature is slightly higher than that of LNG (–160ºC), it is defined on considering temperature raise during transportation in the pipe line between the LNG reservoir and ORV tubes. On the other hand, natural gas outlet temperature 0ºC is the design requirement. Water temperatures at the top of the TE module section 5ºC was calculated using the ORV heat transfer code of Kobe steel. Water temperatures at the bottom of the TE module section 4ºC was given based on the heat transfer coefficient of sea water h_W at the TE module section. LNG temperature at the top of the TE module section –131ºC was obtained by heat transfer code developed by Kobe steel. The module container top temperatures at the top and bottom of the TE module section (0 and –2ºC, respectively) and the module container bottom temperatures at the top and bottom of the TE module section (–120 and –142ºC, respectively) were given by similar procedure as that of equation (2) and (3). Temperature difference between water and the module container top comes from the heat transfer coefficient of sea water h_W. While temperature difference between LNG and the module container bottom is due to thermal resistance of the tube of TE module section as well as the heat transfer coefficient of LNG h_W.

Then operating temperature of the encapsulated TE module in our proposed system is; container hot side –2ºC and cold side –142ºC (ΔT=140 K) at the bottom of the TE module section, and container hot side 0ºC and cold side –120ºC (ΔT=120 K) at the top of the TE module section. Corresponding module power and conversion efficiency are given in the data of CTE test rig as already shown in Fig. 18. However, better performance is expected on adopting type N modules as shown in Table 2. Here we suppose average conversion efficiency of the encapsulated TE module in the TE module section as 4.0%, although it is

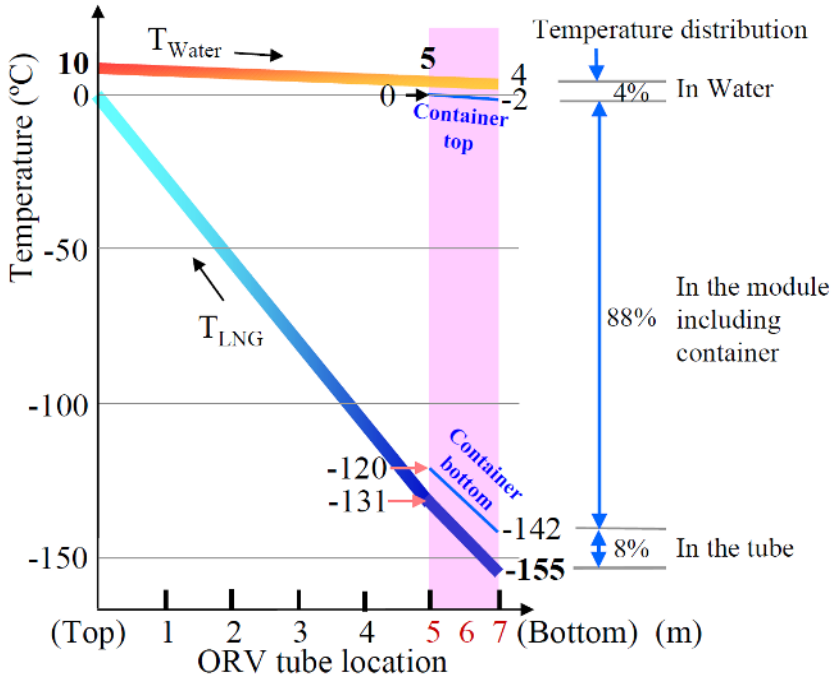

Fig. 20 Calculated temperature distribution in the proposed system

still conservative on considering future improvement of the proposed system as well as TE semiconductor materials.

4.2 System performance

Cold heat released by LNG in the TE module section Q_{LNG} is given as follows.

$$Q_{LNG} = WC_p\Delta T = 2690 \text{ (kW)} \quad \text{--- (7)}$$

where

W: LNG flow rate = 120×10^3 (kg/h) =120×10^3 (kg/h)/3600 (s/h) =33.3 (kg/s)

C_p: Specific heat of LNG =3.36 (kJ/kgK) =3.36 (kWs/kgK)

ΔT: Temperature raise of LNG in the TE module section =155-131=24 (K)

Effective heat transfer area of the TE module section A_{eff} and Q_{LNG} are related by the logarithmic mean temperature ΔT_m.

$$\Delta T_m = \frac{(5+131)-(4+155)}{\ln\left[(5+131)/(4+155)\right]} = 147 \text{ (K)} \quad \text{--- (8)}$$

$$A_{eff} = \frac{Q_{LNG}}{h\,\Delta T_m} = \frac{2690\times10^3 \text{ (W)}}{162.3 \text{ (W/m}^2\text{K)} \times 147 \text{ (K)}} = 112.7 \text{ (m}^2\text{)} \quad \text{--- (9)}$$

where

ΔT_m: Logarithmic mean temperature

A_{eff}: Effective heat transfer area of the TE module section

Q_{LNG}: Cold heat released by LNG in the TE module section

h: System thermal conductance =1/R = $1/6.16\times10^{-3}$ (m^2K/W) = 162.3 (W/m^2K)

Effective heat transfer area A_{eff} coinsides fairly well with that of our analytical model (108 m^2). On adopting above ΔT_m, heat passes through the TE module section Q is estimated as follows.

$$Q = A\,h\,\Delta T_m = 108 \text{ (m}^2\text{)}\times162.3 \text{ (W/m}^2\text{K)}\times147 \text{ (K)} = 2580\times10^3 \text{ (W)} \quad \text{--- (10)}$$

where

A: Heat transfer area of the TE module section (geometrically defined) = 108 (m^2)

A slight difference between Q_{LNG} and Q comes from heat transfer at the transition elements.

Electrical power of the TE system P_{TE} is given as follows.

$$P_{TE} = \eta\, Q_{TE}\, C = 0.66\,\eta\, Q\, C = 63.3 \text{ (kW}_{AC}\text{)} \quad \text{--- (11)}$$

where

η: TE module conversion efficiency (averaged in the TE module section) = 0.04

Q_{TE}: Heat passes through the encapsulated TE modules = 0.66 Q

Q: Heat passes through the TE module section = 2580 (kWt)

C: DC/AC conversion efficiency = 0.93

4.3 Cost evaluation

In this chapter electricity production cost of the proposed TE system which provides 63.3 kW is estimated based on the following assumptions.

Design life of the ORV installation: 20 (years)

Design life of the encapsulated TE modules: 10 (years)

Plant availability: 80 (%)

Encapsulated TE module cost including mounting pieces and connectors: ¥ 1400

Note that the encapsulated TE module is not released in the market yet, above price is CRIEPI's target which could be achieved within a few years. The followings are also necessary for cost evaluation.

Electricity produced in 20 years:

63.3 (kW)×20 (year)×365 (day)×24 (h)×0.8 (plant availability)= 8.87×10^6 (kWh)

Number of encapsulated TE modules:

N=52 (modules)×540 (tubes)=28080 (modules)

As shown in Table 4, electricity production cost of 16 (¥/kWh) is foreseen.

Table 4 Cost breakdown and the electricity production cost

Encapsulated TE modules, mounting pieces and connectors: 28080 (modules)× ¥ 1400× 2 (times)=¥ 80×10^6 Mounting cost of the encapsulated TE modules on the tube: ¥ 4×10^6 ×2 (times) = ¥ 8×10^6 DC/AC converter and electric distributor: ¥ 3×10^6 Additional cost for the ORV tubes with respect to conventional one: ¥ 45×10^6 Additional cost for the ORV building: ¥ 3×10^6
Total cost: ¥ 139×10^6 Electricity production cost: ¥ 139×10^6 / 8.87×10^6 (kWh) = 16 (¥/kWh)

As already discussed in chapter 3.4, N type modules or other advanced modules could provide more electrical power and accordingly reduce the electricity production cost.

5. Investigation of the Sea-water-resistant Module Container

5.1 Requirements on the container material

The encapsulated TE module tested at CTE test rig adopted stainless steel (SUS316) container, however, it is not suitable in view of sea water corrosion. While aluminum alloy ORV tubes are coated by Al-Zn alloy to avoid sea water corrosion. This coating should be done every several years. Because coating is achieved by flame spraying, it is not applied to the encapsulated TE module which is not allowed to heat over 150°C. Hence several candidate materials were tested. Requirements for the container materials are; 1) die formability, 2) machinability, 3) weldability and 4) corrosion resistance to sea water. Materials tested were SUS317L, SUS329J4L and NAS254N. These materials satisfy requirements 1)-3), and then sea water corrosion tests, both in stagnant and stream have been done for the container samples made of these materials.

5.2 Sea-water compatibility test of the candidate materials

Artificial sea water of 30°C was adopted in both stagnant and stream tests. One of the results is shown in Fig.21. SUS329J4L presented the best corrosion resistance. However, crevice corrosion was perceived in all samples. The EDS analyses revealed that corrosion product was oxygen and chlorine composites. It could be possible to avoid crevice in the future container design.

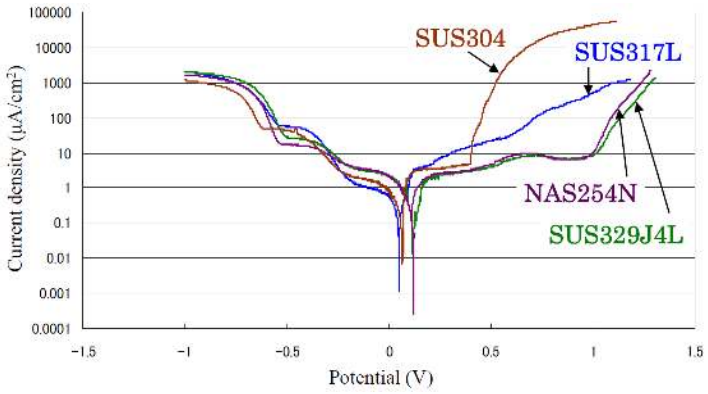

Fig. 21 Polarization curves in artificial sea water (30ºC, 0.4 l/min)

6. Conclusion

A 63 kW TE system design for open rack type LNG vaporizer (120 t/h) has been presented based on the TE module performance test results, and its electricity production cost was evaluated as 16 (¥/kWh). Design policy of this TE system is to get electrical power without any influence on the ORV performance. In addition it should be as compatible as that of conventional ORV so as that this TE system is easily introduced in the market.

The next step of research and development should be focused to the test using prototype test rig consists of multi-ORV tubes in which not liquefied nitrogen but LNG passes through. An advanced encapsulated TE module could provide more electrical power and accordingly reduce the electricity production cost.

Acknowledgments

The authors wish to acknowledge the contribution of H. G. Mayer, H. J. Menz and R. Marschall of KE-Technologie GmbH of the Stuttgart University for their assistance in executing experiments.

References

[1] Shikata, H. and Kambe, M., "Development of Advanced Thermoelectric System for Belt-driven Furnaces and Incinerators," NEDO Technical Report, 2007, http://www.tech.nedo.go.jp/servlet/HoukokushoKensakuServlet?db=n&kensakuHoho=Barcode_Kensaku&SERCHBARCODE=100010933.

[2] Goto, M., Shinkai, K., Egashira, S. and Konishi, K., "SUPERORV Development and Marketing," R-D Kobe Steel Engineering Reports, Vol. 53, No. 2, September 2003.